Pharmacogenomics and Personalized Medicine

Dovepress

open access to scientific and medical research

Open Access Full Text Article

ORIGINAL RESEARCH

Microarray Expression Profile and Bioinformatic Analysis of Circular RNA in Human Arteriosclerosis Obliterans

Yu Zhou[1,*], Huoying Cai[1,*], Lin Huang[1,*], Mingshan Wang[1], Ruiming Liu[2], Siwen Wang[1], Yuansen Qin[1], Chen Yao[1], Zuojun Hu[1]

[1]Division of Vascular Surgery, National-Guangdong Joint Engineering Laboratory for Diagnosis and Treatment of Vascular Disease, The First Affiliated Hospital, Sun Yat-sen University, Guangzhou, People's Republic of China; [2]Laboratory of Department of Surgery, The First Affiliated Hospital of Sun Yat-sen University, Guangzhou, People's Republic of China

*These authors contributed equally to this work

Correspondence: Zuojun Hu; Chen Yao, Email huzuojun@mail.sysu.edu.cn; yaochen@mail.sysu.edu.cn

Background: Arteriosclerosis obliterans (ASO) is the leading cause of nontraumatic lower-extremity amputations. Multiple researches have suggested that circular RNAs (circRNAs) played vital regulatory functions in cancer and cardiovascular disease. Nevertheless, the underlying effect and pathological mechanism of circRNAs in the formation and progression of ASO are still indistinct.

Methods and Results: This study used microarray analysis to investigate the expression portrait of circRNAs in normal lower extremity arteries and ASO arteries. Bioinformatics analysis was conducted using the KEGG database to study the enrichment of differentially expressed circRNAs (DE circRNAs) and predict their functions. The accuracy of microarray assay was verified by evaluating expression of the top 5 upregulated and 5 downregulated circRNAs (raw density of normal group ≥200) using RT-qPCR. A circRNA-miRNA-mRNA interaction network was further predicted using software. Compared to the normal lower extremity group, the ASO arteries with HE and EVG staining presented hyperplastic fibrous membrane and luminal stenosis. A total of 12,735 circRNAs were identified, including 1196 DE circRNAs with 276 upregulated and 920 downregulated in ASO group based on |log2 (FC)| > 1 and padj < 0.05. Among selected 10 circRNAs, RT-qPCR confirmed that hsa_circ_0003266, hsa_circ_0118936 and hsa_circ_0067161 were upregulated while hsa_circ_0091934 and hsa_circ_0092022 were downregulated in ASO group ($p < 0.05$). GO analysis presented that the DE circRNAs were primarily enriched in protein binding, intracellular part and organelle organization. KEGG pathway analysis indicated that MAPK signaling pathway, human T-cell leukemia virus 1 infection, proteoglycans in cancer were associated with the DE circRNAs. The circRNA-miRNA-mRNA interactive network revealed that both mRNAs and miRNAs linked to circRNAs played an indispensable role in ASO.

Conclusion: This study described the expression portrait of circRNAs in human ASO arteries, and revealed the molecular background for further investigations of the circRNA regulatory mechanism in the formation and progression of ASO.

Keywords: arteriosclerosis obliterans, circular RNA, gene ontology analysis, pathway analysis, circRNA-miRNA-mRNA interaction network

Introduction

Arteriosclerosis obliterans (ASO) is a chronic disorder with atherosclerosis involving lower extremity arteries leading to arterial stenosis or occlusion. The incidence continues to increase with age, affecting about 202 million people worldwide to varying degree.[1–3] Despite the proposed theories of lipid infiltration, arterial intimal injury, and chronic inflammation, the molecular mechanism underlying ASO pathogenesis remains unclear.[4]

As a kind of non-coding RNA, circRNAs (CircularRNAs, circular RNA molecule) are characterized by the deletion of 5'- terminal cap and 3'- terminal poly (A) tail and circular covalently closed structure. Due to the circular structure,

Received: 29 July 2023
Accepted: 16 October 2023
Published: 24 October 2023

circRNAs are resistant to RNase degradation and have greater stability in vivo.[5] Recently, some studies have suggested that circRNAs played essential molecular regulated roles in diabetes, neuropathy, cardiovascular disease and cancer.[6–8] For example, through the *FUS/VEGF-A* axis, *CircFndc3b* promoted cardiac repair after myocardial infarction.[9] Circular RNA *Cdyl* induced M1 polarization of macrophage and aggravated vascular inflammation to accelerate the formation of abdominal aortic aneurysm by inhibiting the nuclear translocation of interferon regulatory factor 4 (*IRF4*).[10] However, the substantial function and regulatory mechanism of circRNAs in the formation and progression of ASO remain rarely clear.

In the current study, we collected and detected the expression of circRNA in human normal lower extremity arteries and ASO arteries to describe the circRNA expression profile in ASO patients. This study laid a molecular foundation for elucidating the pathogenesis, identifying therapeutic targets, and developing early predictive diagnostic and biomarkers for ASO, thereby providing substantial theoretical significance and application value.

Materials and Methods

Sample Attainment

The flowchart outlining the study can be found in Figure 1. Approved by the Research Ethics Committee of the first affiliated Hospital of Sun Yat-sen University (authorized number: [2022]235), this study followed by the Helsinki Declaration. With the consent of donors or their family members, the ASO artery specimens were taken from lower limb amputation specimens of three patients with severe ASO, and normal arterial samples were taken from three normal donors without ASO. The obtained vascular tissues, approximately 3 cm in length, were divided into two sections. One half was fixed with paraformaldehyde (4%) for subsequent morphology observation. The other half was frozen in liquid nitrogen followed by RNA extraction.

Histological Observation

Three ASO arterial samples and three normal lower extremity arterial tissues were acquired and fixed in paraformaldehyde (4%). After dehydrated by alcohol, samples were subsequently embedded in paraffin wax for 5-μm sections. Next, hematoxylin (blue) and eosin (pink) were adopted to stained and presented the nuclei and cytoplasm, respectively. Medial elastin destruction was evaluated by Verhoeff-Van Gieson (Biosci, China). Finally, the tissue sections were observed under a 10X or 20X microscope (Olympus, Japan) to identify any histological alterations. The severity of medial elastin degradation was evaluated as previously described:[11,12] grade 1, no degradation; grade 2, mild elastin degradation; grade 3, severe elastin degradation; grade 4, aortic rupture.

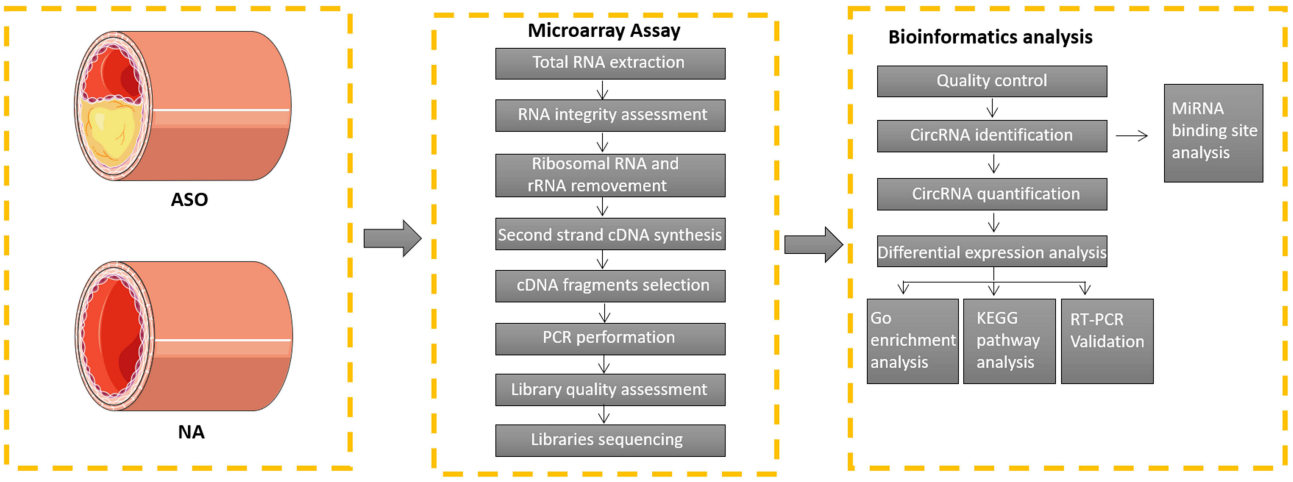

Figure 1 Analytical process of this study.

Microarray Assay

The circRNA expression portrait of normal lower extremity arterial (n = 3) and ASO (n = 3) was characterized at KangChen Bio-tech (Shanghai, China) using an Arraystar Human Circular RNA Array V2 analysis. Concisely, after extracting by TRIzol reagent (Invitrogen, Co. Ltd), total RNA of arterial tissues snap-frozen in liquid nitrogen were performed on 1% agarose gels to exclude degradation and contamination. In order to eliminate linear RNAs completely and purify circRNAs, the quantified RNA of each sample was processed with the RNase R (Epicentre, Inc). Next, RNA was fragmented and reverse transcripted into fluorescent cRNA with an Arraystar Super RNA Labeling Kit (Arraystar) in a random primer method. The labeled cRNAs (pmol Cy3/μg cRNA) was enriched according to a RNeasy Mini Kit (Qiagen), and the specific activity and concentration were measured by NanoDrop ND-1000 (Thermo Scientific, United States). Each labeled cRNA was fragmented for 30 minutes at 60°C after it was mixed with recommended fragmentation buffer and blocking agent. Diluted with 25 μL hybridization buffer, the mixture was then dispensed into the gasket slide and gathered to the circRNA sequencing slide for incubation at 65°C for 17 hours in the Agilent Hybridization Oven. Agilent Feature Extraction software (version 11.0.1.1) was applied to profile array images acquired after washing the slides with the Agilent Scanner G2505C. All the primary and processed sequencing data originated from this study were uploaded to the NCBI Gene Expression Omnibus (GEO) database (GSE152280).

Identified DE circRNAs

The R software limma package was adopted to evaluate the expression difference between the two groups. The *p* value was adjusted by Benjamini and Hochberg to control the error detection rate. Differentially expressed circRNAs were determined as possessing adjusted *p* value found by limma package. Significant differentially expressed circRNAs were designated as those with $|\log2(\text{fold change})| > 1$ and $padj < 0.05$.

Gene Ontology and KEGG Pathway Enrichment Analysis of circRNAs

GO analysis was implemented by the R package "Goseq" to identify the host genes of differentially expressed circRNAs, in which gene length deviation was rectified. GO terms with threshold $p < 0.05$ as well as those with adjusted $p < 0.05$ were supposed to be significantly enriched in genes with differential expression. Additionally, pathway enrichment analysis for host genes of differentially expressed circRNA was performed using the R package "Cluster Profiler" based on KEGG analysis. Pathways were significantly enriched if they had an adjusted *p* value less than 0.05. Histograms and bubble charts illustrated the top ten significantly enriched GO terms and signal pathways of differentially expressed genes, respectively.

Quantitative Reverse Transcription PCR Validation

The top 5 up-regulated and 5 down-regulated circRNA (raw density of the normal group ≥200) were selected to measure by quantitative real-time PCR, as shown in Table 1. Three ASO arterial samples and three normal lower extremity arterial tissues were acquired for RNA acquisition according to the Trizol method (Invitrogen, Co. Ltd). Then, synthesis of cDNA was performed using an All-in-One First-Strand cDNA Synthesis Kit (GeneCopoeia, Inc, Cat. No. QP007, China) in accordance with the instructions of manufacturer. Next, RT-qPCR was carried out using the BlazeTaq SYBR® Green qPCR mix 2.0 kit (GeneCopoeia, Inc, Cat. No. QP041, China) to detect the expression of the selected circRNAs, with GAPDH used as the internal reference gene. The relative circRNA expression was calculated by $2^{-\Delta\Delta Ct}$ method. Table 2 presents the specific primers used in the current study.

miRNA Target Prediction and Functional Enrichment Analysis

The differentially expressed circRNAs were selected to identify miRNA binding site in the exons and hereby establish the miRNA-mRNA network according to the total integral and energy values of the predicted binding sites of all targets by Miranda software. Finally, Cytoscape software was adopted to create a predictive circRNA-miRNA-mRNA interactive network.

Statistics

The experimental data in this study were shown as mean ± SD. After performing a normal distribution test for all continuous variables and confirmation of the variance equality between different groups, significant differences between two

Table 1 The Most Significantly 5 Up-Regulated and 5 Down-Regulated circRNAs (Raw Density of the Normal Group ≥200) in Microarray Analysis

ID	NC Readcount	ASO Readcount	Log2FC	Pavl	Padj
hsa_circ_0044097	1912.5	507.166667	4.0372972	0.001255	0.0139375
hsa_circ_0003266	1295.666667	417.166667	3.6559456	0.0008921	0.0130497
hsa_circ_0118936	1061.666667	333.666667	3.648185	0.0153102	0.0434825
hsa_circ_0092303	4272.333333	1250.666667	3.1383759	0.0086705	0.0309818
hsa_circ_0067161	1372.666667	514.333333	3.0774146	0.0001848	0.0096161
hsa_circ_0091934	380	8823.833333	29.338455	0.0002999	0.0110373
hsa_circ_0050900	349.166667	7802.666667	27.267452	0.001487	0.0145583
hsa_circ_0007386	147	4375.5	27.167938	0.0005477	0.0117977
hsa_circ_0050898	983.333333	18,144.83333	26.551027	0.0009403	0.0131719
hsa_circ_0092022	192	4946.833333	25.854846	0.0004893	0.0116737

Table 2 The Primer Sequences Used for RT-qPCR (from 5' to 3')

Gene		Sequence 5'- 3'
hsa_circ_0044097	Forward	CTGATCTCCGGACTCACACC
	Reverse	CCTTCTCAAGAGGCTCAGCA
hsa_circ_0003266	Forward	GCTGCTTCATCACATGTCGT
	Reverse	GCAAGTCCTCAAAACCAGCA
hsa_circ_0118936	Forward	TGTATCTCCAGGGCAGCTTACT
	Reverse	TTGGATGGTCAGAAGGGTTTG
hsa_circ_0092303	Forward	CATCATCACAGCCCCTCCC
	Reverse	ACTTCCCACTTAAGCCCCTC
hsa_circ_0067161	Forward	ACCCAGGGTCCGGTACTG
	Reverse	AGGAAGAGCACATTGGGGAT
hsa_circ_0091934	Forward	GGAGAATGAGGACGGCACTT
	Reverse	CCTTCGGGATCCGTCACTT
hsa_circ_0050900	Forward	ATACCTCGACATCCCCAAGA
	Reverse	TGTTCTCGATCTGTGTGCCT
hsa_circ_0007386	Forward	GTTGCTGTACTTTGCCAACAA
	Reverse	ACGTGGAGAGAACTGGACTT
hsa_circ_0050898	Forward	AGGTCTTAGCAGGGGACAA
	Reverse	TAGTCCACCATTCCGCCG
hsa_circ_0092022	Forward	ATCGCCAACAAGACCACCTA
	Reverse	TAAAGTCGCAGGCACCTAGG
GAPDH	Forward	ACAACTTTGGTATCGTGGAAGG
	Reverse	GCCATCACGCCACAGTTTC

independent groups were evaluated by unpaired Student's *t*-test, whereas significant differences between multiple groups were analyzed using one-way ANOVA with a post Bonferroni's multiple comparisons test. For variables with a non-normal distribution, a nonparametric Mann–Whitney test for two independent groups was applied. P-values less than 0.05 were determined as statistically significant when analyzed by SPSS 25.0 (IBM Corporation, Armonk, NY, USA).

Results

Histopathology

As shown in Figure 2A, the ASO arterial samples presented the following characteristics compared to the normal lower extremity arteries: the intima of the plaque surface was destroyed, and the lipid pool was covered by a hyperplastic fibrous membrane (fibrous cap), lesions expanded to the media and destroyed the arterial wall resulting in fibrous

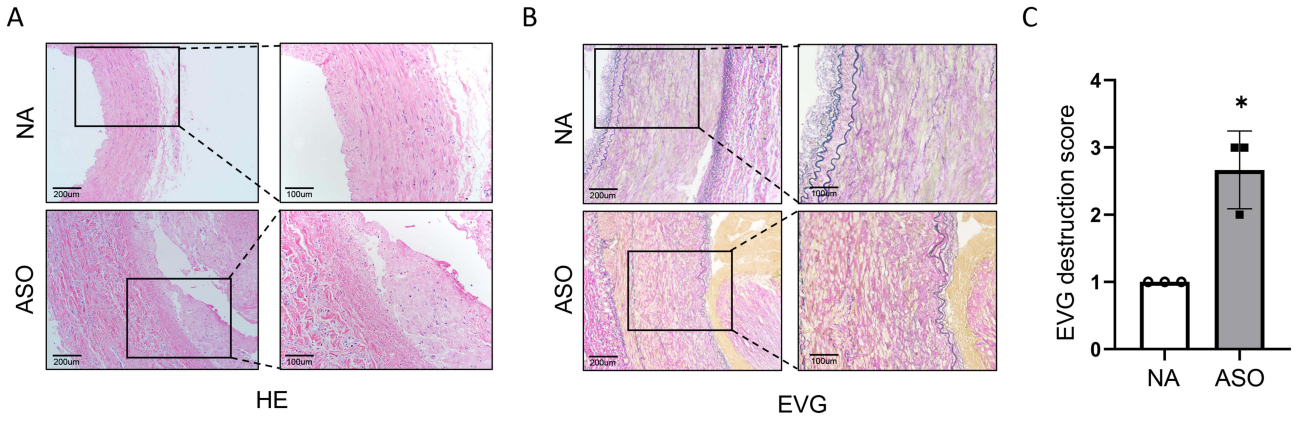

Figure 2 (**A** and **B**) The histopathology features of HE and EVG stained normal and ASO arterial tissues sections. (**C**) Medial elastin destruction was graded as I (mild) to IV (severe).
Notes: Scale bar = 100 and 200 μm. Nonparametric Mann–Whitney test, *$p < 0.05$ NC vs ASO, n=3/group. EVG, Verhoeff's Van Gieson.

connective tissue hyperplasia, degeneration and other secondary lesions, hereby leading to luminal stenosis. In EVG staining, the degree of elastin destruction, as evaluated by histological scores, was significantly aggravated in ASO arterial samples as compared with normal lower extremity arteries ($p < 0.05$, Figure 2B and C).

circRNA Expression Portraits

Microarray sequencing assay recognized totally 12,735 circRNAs from the ASO group and normal group. According to the threshold criteria of $|\log2(FC)| > 1$ and padj < 0.05, a total of 1196 DE circRNAs, including 276 upregulated and 920 downregulated circRNAs, were identified. To further present the relative expression of DE circRNAs in the two groups, a heatmap (Figure 3A) and volcano map (Figure 3B) were drawn based on the threshold of log2FC and -log10p. The top 5 most prominently upregulated and downregulated circRNAs (raw density of the normal group ≥200) are shown in Table 1.

circRNA Gene Symbols and Pathway Analysis

Both GO and KEGG pathways analyses were performed to explore the potential biological function of module genes. Figure 4A illustrates the top 10 items at three gene ontology levels (biological processes,[13] molecular function[14] and cell component). Specifically, circRNAs with differential expression were mainly enriched in protein binding, binding and heterocyclic compound binding in molecular function.[13] As for cell component,[14] the most enriched items were intracellular part, cytosol and intracellular organelle. In terms of biological processes enriched highly in the DE circRNAs, organelle organization, developmental process, and anatomical structure development were identified. According to KEGG pathway analysis (Figure 4B), DE circRNAs were primarily associated with biological pathways such as focal adhesion, MAPK signaling pathway, proteoglycans in cancer, transcriptional misregulation in cancer, human T-cell leukemia virus 1 infection, insulin signaling pathway, AGE-RACE signaling pathway in diabetic complications, adherents junction, ErbB signaling pathway and pancreatic cancer.

RT-qPCR Validation

The top 5 upregulated and 5 downregulated circRNA (raw density of normal group ≥200) were in-depth confirmed by RT-qPCR on three ASO arterial samples and three normal lower extremity arteries. Compared to the normal group, three circRNAs (hsa_circ_0003266, hsa_circ_0118936 and hsa_circ_0067161) were highly expressed while hsa_circ_0091934 and hsa_circ_0092022 were considerably downregulated in the ASO group ($p < 0.05$). These proven outcomes revealed that the majority of identified circRNAs by the microarray assay were dependable and deserved further research (Figure 5).

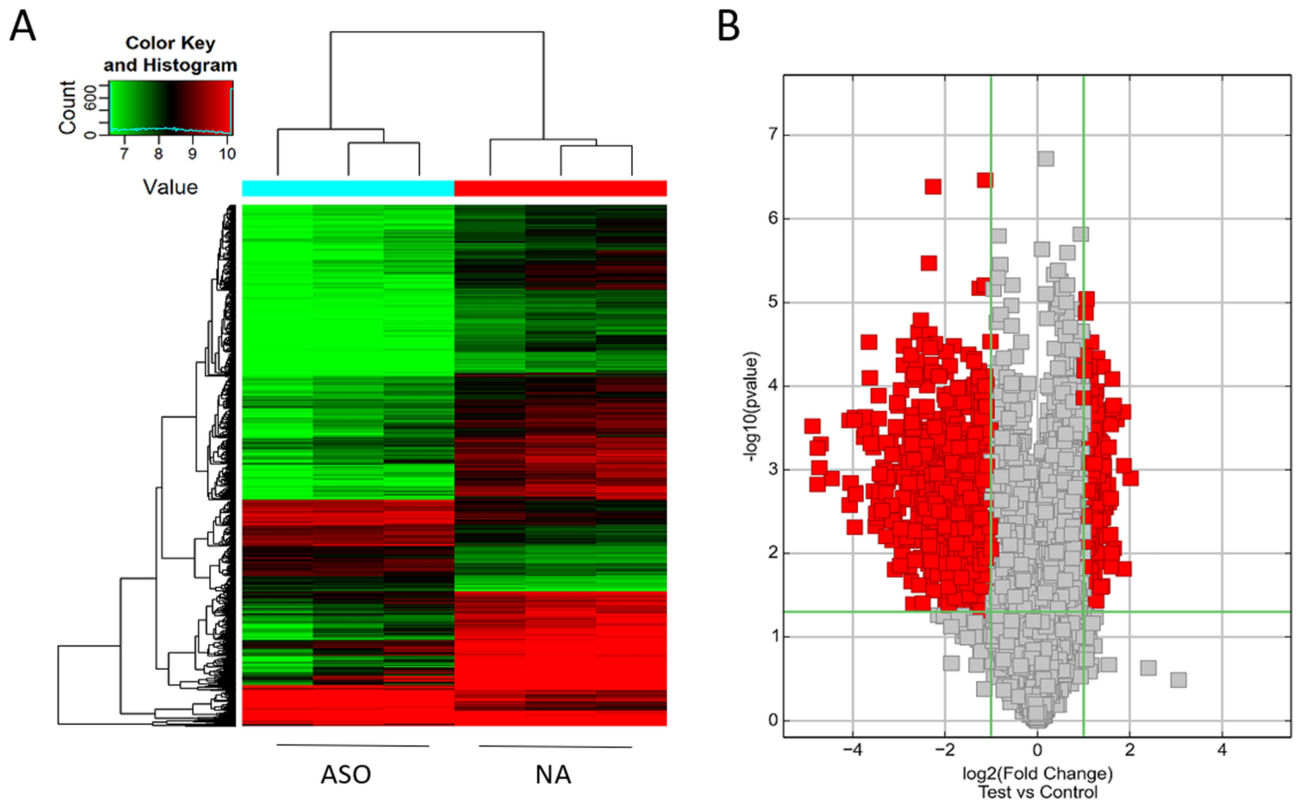

Figure 3 Differentially expressed circRNAs between normal and ASO arterial tissues.
Notes: (**A**) Heat map showed the DE circRNAs in normal and ASO arterial tissues. The circRNA-seq samples (X-axis) were hierarchically clustered based on expression similarity profiles at the top. On the left (Y-axis) means DE circRNAs, which were clustered based on the expression similarity. Colour differed from green to red with green denoting relatively downregulated expression and red representing relatively up-expressed circRNAs. (**B**) Volcano plot exhibits the DE circRNAs in normal and ASO arterial tissues. The log2 fold-change of circRNA expression between the ASO and normal group was represented on the X-axis, and the statistically significant degree of various circRNA expression change was represented on the Y-axis. Each scattered box in the plot represented the expression value for each circRNA, the gray boxes meant no significant difference of circRNAs expression, and the red boxes represented the significantly expressed circRNAs.

Prediction of circRNA-miRNA-mRNA Network for Each circRNA

To further investigate and portrait the underlying roles of DE circRNAs in ASO, miRanda was used to explore and predict the target miRNAs and mRNAs of the five circRNAs (hsa_circ_0003266, hsa_circ_0118936, hsa_circ_0067161, hsa_circ_0091934 and hsa_circ_0092022), which had been validated by RT-qPCR. According to the targeting relationship and target prediction score of the binding site, the top 5 miRNAs probably binding to each circRNA and the 50 target genes were presented (Figure 6). Please see Supplementary Table 1 for detailed information of target genes.

Discussion

Arteriosclerosis obliterans is a systemic arteriosclerotic disease in the lower extremities, which is characterized by the involvement of large and middle arteries, mostly in elderly patients.[2,15] Generally, the atherosclerotic artery wall will experience mainly four phase pathological progress, including lipid stripes, fibrous plaques, atherosclerotic plaques and secondary lesions.[16,17] On the basis of lipid metabolism disorder, atherosclerosis is marked by intima beginning, followed by accumulation of lipids, hemorrhage and thrombosis, fibrous tissue hyperplasia and calcareous precipitation, medial calcification, resulting in arterial stiffness and luminal stenosis.[18,19] It is called atherosclerosis for the reason of the lipid accumulation and plaque hardening in the artery intima. Mostly, the pathological manifestations of arteriosclerosis obliterans are caused by thrombosis regardless of the extent of atherosclerosis.[18,20] In this study, the ASO sample showed a stable phenotype, and fibrous plaque played a dominant role in severe atherosclerosis of lower extremity arterial.

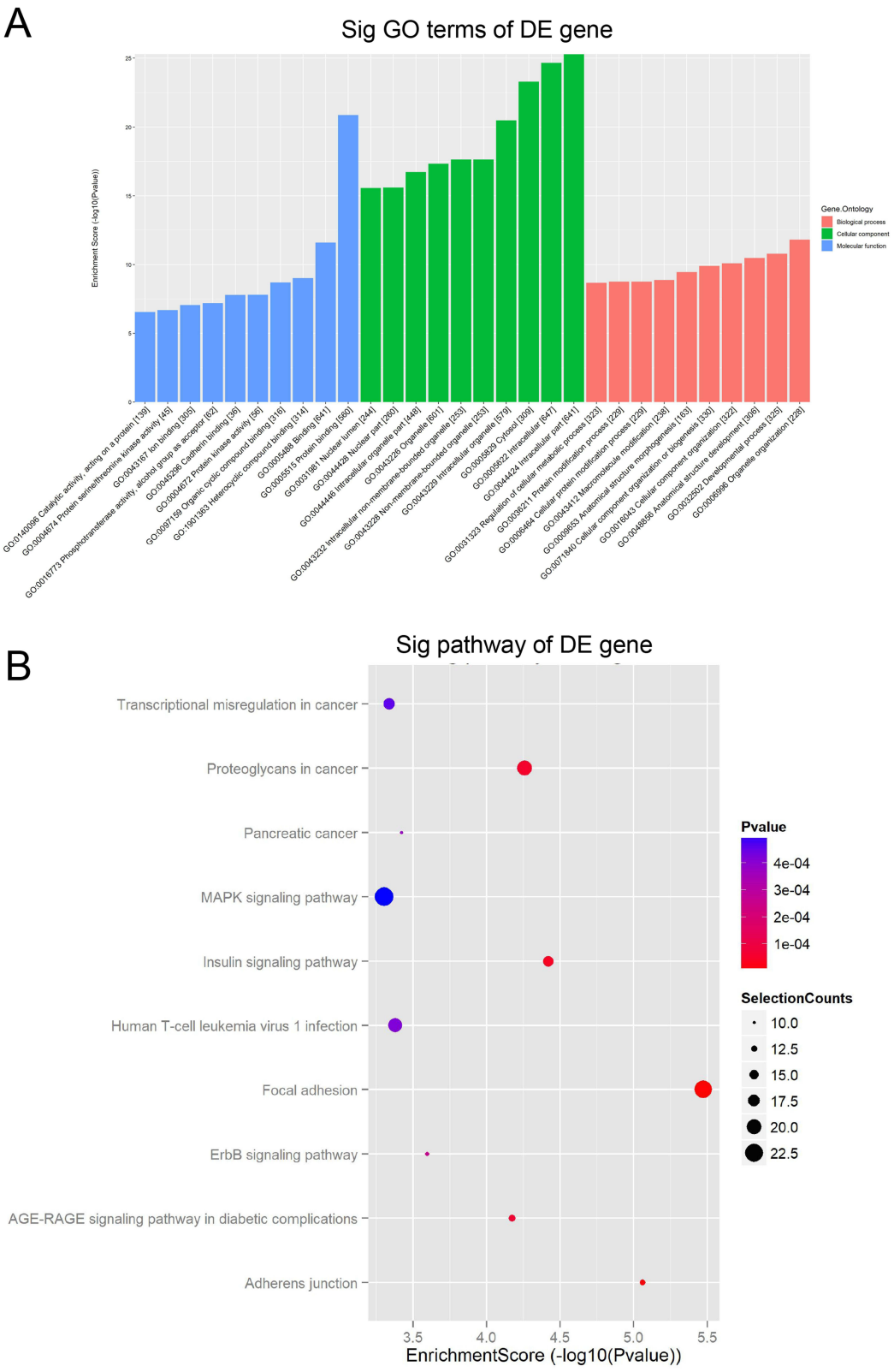

Figure 4 The results of GO and KEGG analysis.

Notes: (**A**) The top 10 GO terms of DE circRNA host genes at three gene ontology levels (biological processes, molecular function and cell component). (**B**) The top 10 signal pathways of KEGG pathway enrichment analysis. The enrichment score of each pathway was represented on X-axis while the pathway name was represented on Y-axis. The size of the dots reflected the selection counts, and the color was consistent with the different p value ranges.

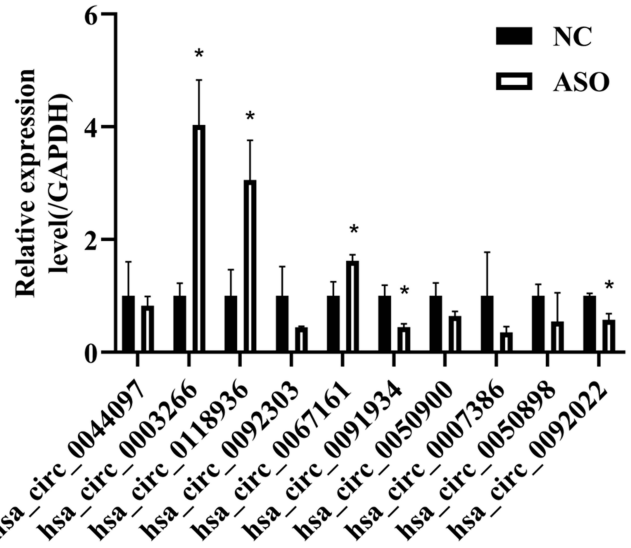

Figure 5 Validation of microarray assay results by RT-qPCR of 10 selected circRNAs (the top 5 upregulated and 5 downregulated circRNAs, raw density of the normal group ≥200).

Notes: Sequencing-detected changes of the 10 selected circRNAs were confirmed using RT-qPCR in the normal and ASO arterial tissue groups (n = 3). Bars show means ± standard deviation. Bars show the mean and error bars the standard deviation. *$p < 0.05$ NC vs ASO.

CircRNA is a conservative endogenous product generated by back-splicing, distinguished by a covalent closed loop structure.[6,8,21] Many circRNAs are evolutionarily conserved and highly abundant in eukaryotes, and they mainly perform crucial biological functions in the following way: acting as "sponges" to inhibit the microRNA or protein, regulating protein function directly, being translated themselves.[6,8,21,22] Some studies have revealed the emerging roles of circRNAs in cell proliferation, immune responses regulation, and metabolism processes.[8,23] However, there are few reports about circRNA expression changes and regulatory network in ASO. Using microarray assay, 276 upregulated and 920 downregulated circRNAs were distinguished in the present study. Among them, the top 5 upregulated and 5 downregulated circRNAs (raw density of normal group ≥200) were selected for RT-qPCR validation. As a result, 5 circRNAs expression were in accord with those of microarray assay, indicating that the expression of circRNA has changed in ASO. According to the literature, hsa_circ_0003266 was upregulated in the plasma of patients with type 2 diabetes mellitus combined with proliferative diabetic retinopathy,[24] hsa_circ_0118936 was upregulated in the plasma of patients with primary biliary cholangitis,[25] and hsa_circ_0091934 was a diagnostic marker for congenital heart disease.[26] In this study, hsa_circ_0003266 and hsa_circ_0118936 were upregulated in the ASO vascular tissue, while hsa_circ_0091934 was downregulated, suggesting that these three circular RNAs may also be potential diagnostic or prognostic markers for ASO. As for hsa_circ_0067161 and hsa_circ_0092022, there are no studies on their relationship with the disease, so further research on their relationship with ASO is interesting. Based on sequencing results, 50% of differentially expressed circular RNA was validated with RT-qPCR. This may be due to the fact that the gene expression patterns of ASO differ at different stages of development. ASO is a heterogeneous disease, and there may be different molecular subtypes or circular RNA-specific subtypes that need to be further explored. Furthermore, due to the limited number of sequencing and experimental validation samples, as well as the fact that the tissue samples used for sequencing and experimental validation were not taken from the same patients, the validation results may differ from the sequencing results. Overall, this study successfully confirmed the presence of five differential circRNAs that have not been previously explored in the context of ASO diseases. However, further comprehensive investigations are warranted to delve into the specific roles played by them in ASO diseases.

At present, the occurrence and development of ASO was explained by mainly the following mechanisms. Firstly, lipid hypothesis believes that the permeability of vascular wall changes due to endothelial cell injury, focal exfoliation and plasma lipoprotein enter the intima, resulting in macrophage clearance reaction, vascular wall smooth muscle cell proliferation and plaque formation.[27–29] The second one is vascular endothelial damage-response theory caused by

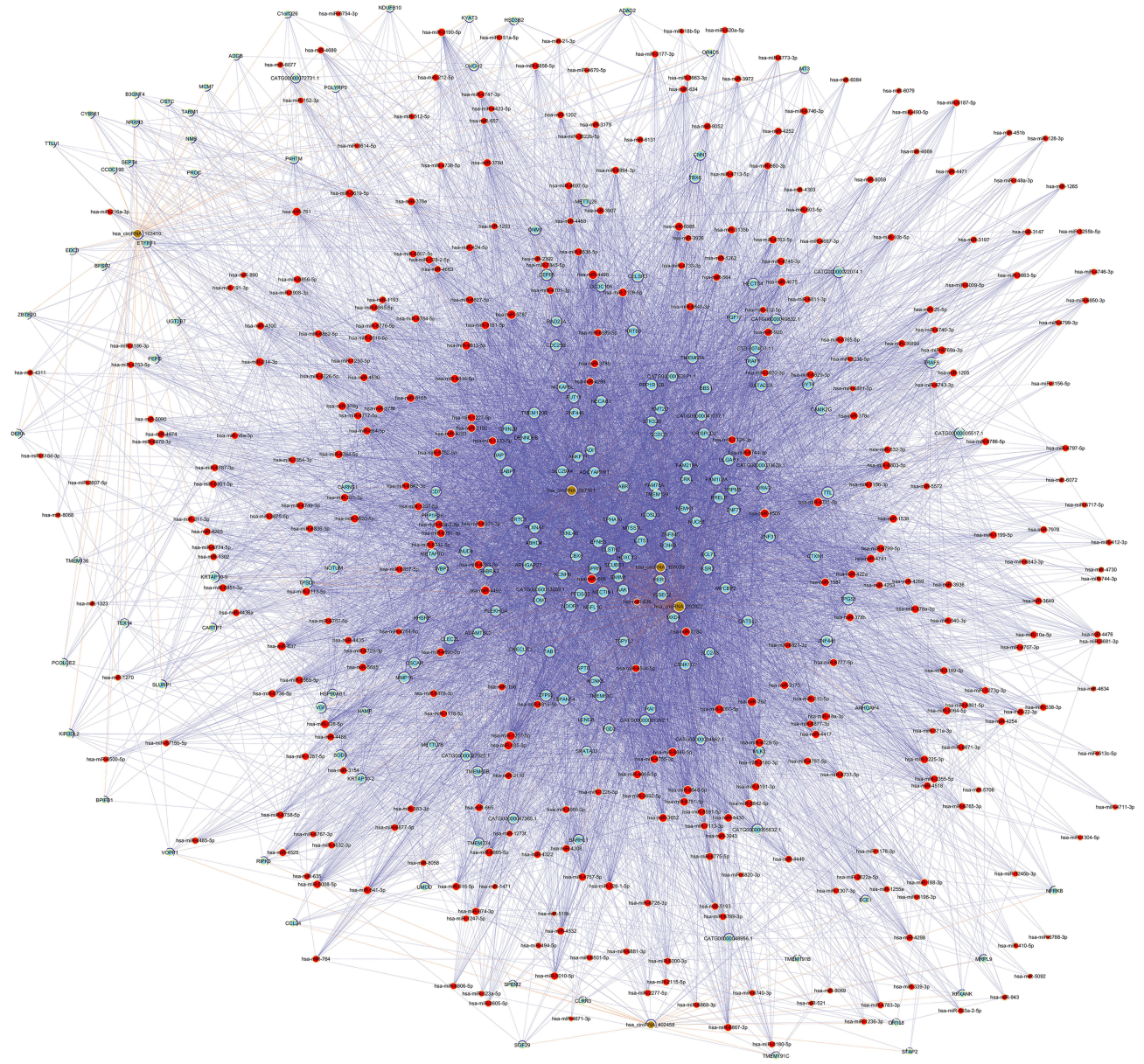

Figure 6 The construction of circRNA-miRNA-mRNA network.
Notes: Based on the ceRNA (circRNA-miRNA-mRNA) interaction information from Cytoscape, 5 validated and consistent circRNAs (hsa_circ_0003266, hsa_circ_0118936, hsa_circ_0067161, hsa_circ_0091934 and hsa_circ_0092022) were annotated in detail. According to the prediction outcome of miRNA and mRNA, the top 5 miRNAs may be regulated by these 5 validated circRNAs, and the top 50 target genes of each miRNA were presented. Brown: circRNAs. Red: miRNAs. Blue: mRNAs.

mechanical interference, exposure to toxins, or endogenous inflammatory signals and so on. Once endothelial injured, Low-density lipoprotein (LDL) and other plasma factors accumulate and platelets adhere at the injury site. Subsequently, vascular smooth muscle cells are stimulated to proliferate, migrate and form thickened neointima by α particles released by platelets, resulting in arterial lumen stenosis.[30,31] The third mechanism – inflammation theory holds that inflammation is the core of atherosclerosis.[32] A range of inflammatory cytokines and various growth factors, such as monocyte chemoattractant protein-1 (*MCP-1*), interleukin-1 (*IL-1)*, interleukin-3 (*IL-3)* interleukin-6 (*IL-6)* and interleukin-18 (*IL-18)*, tumor necrosis factor-α (*TNF-α*) are synthesized and secreted by arterial wall cells and macrophages-monocytes under certain conditions, leading to inflammation and atherosclerosis.[33–35] Fourthly, the hemodynamic theory holds that blood flow changes and low shear stress may be involved in the occurrence of atherosclerosis.[36] In the case of hemodynamic changes, the continuity between arterial intimal endothelial cells is interrupted, and then platelets adhere

and gather on the intima, forming mural thrombus. Cytokines, released by platelets and macrophages, enter the arterial wall and accelerate the phenotype switching, proliferation and migration of smooth muscle cells in atherosclerotic lesions.[37]

The fact that circRNAs participated in the inflammation regulation, oxidative stress and signal transduction pathways, relating to diabetes, neuropathy, and cancer, has been confirmed by a variety of studies.[21,22,38] In addition, it was reported that circRNAs were associated with cardiovascular disease, including ASO.[7,39] Similarly, the present study found differential expression of circRNAs in ASO. Bioinformatics analysis was used to further predicted the possible mechanism of circRNAs. According to the result of GO analysis, circRNAs were involved in a variety of cellular biological function, such as protein binding, intracellular part, organelle organization and other processes. Several studies have confirmed that circRNAs were associated with inflammation and oxidative stress by regulating protein binding and metabolism.[8,23,40,41] So, we presumed that circRNAs may participate in the process of ASO by affecting inflammation and oxidative stress through protein binding and metabolism. As for KEGG enrichment analysis, the DE circRNAs were mainly enriched in metabolism relevant pathways, including MAPK signaling pathway, AGE-RACE signaling pathway in diabetic complications and Insulin signaling pathway, which were equal to the GO analysis. Therefore, it was likely that circRNAs could regulate the formation and progression of ASO by participating and modulating these signal pathways. As an inhibitor of miRNAs, circRNAs usually regulate the target gene expression to promote cellular biological function by adsorbing multiple miRNAs.[42–44] In order to better explore possible mechanism, Miranda was applied to predict the target miRNAs and mRNAs of the selected five circRNAs. Massive miRNA binding sites were found and all these five circRNAs regulate the relevant target genes via the ceRNA (competing endogenous RNA) mechanism. Moreover, some of these targeted prediction miRNAs were reported in ASO. However, further study is warranted to verify the correlation of circRNA-miRNA-mRNA interactive network in ASO.

Through sequencing and RT-qPCR validation, five circular RNAs with specific expression in ASO tissues were identified. However, further experimental studies are needed to investigate their roles in the diagnosis and treatment of ASO, due to the limited sample size.

Conclusion

To sum up, the circRNA expression profile of the ASO arterial tissue was described in the present study. Further efforts are urgent to determine the specific roles and the underlying molecular mechanisms of these identified circRNAs in ASO.

Abbreviations

ASO, Arteriosclerosis obliterans; CircRNA, Circular RNA; miRNA, MicroRNA; SFA, Superficial femoral artery; ceRNA, Endogenous competitive RNA; DEGs, Differentially expressed genes; GO, Gene Ontology; BP, Biological processes; MF, Molecular function; CC, Cell component; KEGG, Kyoto Encyclopedia of Genes and Genomes; GEO, Gene Expression Omnibus.

Data Sharing Statement

The dataset of the raw and processed sequencing data originated from this study is freely available from the online repositories: National Center for Biotechnology Information (NCBI) Gene Expression Omnibus (GEO) database (GSE152280).

Ethics Statement

Followed by the Helsinki Declaration, this study was approved (authorized number: [2022]235) by the Research Ethics Committee of the first affiliated Hospital of Sun Yat-sen University.

Funding

This work was funded by the National Natural Science Foundation of China (No: 82000448) to YZ and College Teacher Characteristic Innovation Research Project (2021DZXX11) to ZH.

Disclosure

The authors report no conflicts of interest in this work.

References

1. Song P, Rudan D, Zhu Y, et al. Global, regional, and national prevalence and risk factors for peripheral artery disease in 2015: an updated systematic review and analysis. *Lancet Global Health*. 2019;7:e1020–e1030. doi:10.1016/S2214-109X(19)30255-4
2. Virani SS, Alonso A, Aparicio HJ, et al. Heart disease and stroke statistics-2021 update: a report from the American Heart Association. *Circulation*. 2021;143:e254–e743. doi:10.1161/CIR.0000000000000950
3. Hiatt WR, Goldstone J, Smith SC, et al. Atherosclerotic peripheral vascular disease symposium II: nomenclature for vascular diseases. *Circulation*. 2008;118:2826–2829. doi:10.1161/CIRCULATIONAHA.108.191171
4. Libby P. The changing landscape of atherosclerosis. *Nature*. 2021;592:524–533. doi:10.1038/s41586-021-03392-8
5. Ling Y, Zheng Q, Zhu L, et al. Trend analysis of the role of circular RNA in goat skeletal muscle development. *BMC Genomics*. 2020;21:220. doi:10.1186/s12864-020-6649-2
6. Kristensen LS, Andersen MS, Stagsted LVW, et al. The biogenesis, biology and characterization of circular RNAs. *Nat Rev Genet*. 2019;20:675–691. doi:10.1038/s41576-019-0158-7
7. Zhao G. Significance of non-coding circular RNAs and micro RNAs in the pathogenesis of cardiovascular diseases. *J Med Genet*. 2018;55:713–720. doi:10.1136/jmedgenet-2018-105387
8. Chen LL. The expanding regulatory mechanisms and cellular functions of circular RNAs. *Nat Rev Mol Cell Biol*. 2020;21:475–490. doi:10.1038/s41580-020-0243-y
9. Garikipati VNS, Verma SK, Cheng Z, et al. Circular RNA CircFndc3b modulates cardiac repair after myocardial infarction via FUS/VEGF-A axis. *Nat Commun*. 2019;10:4317. doi:10.1038/s41467-019-11777-7
10. Song H, Yang Y, Sun Y, et al. Circular RNA Cdyl promotes abdominal aortic aneurysm formation by inducing M1 macrophage polarization and M1-type inflammation. *Mol Ther*. 2022;30:915–931. doi:10.1016/j.ymthe.2021.09.017
11. Song H, Xu T, Feng X, et al. Itaconate prevents abdominal aortic aneurysm formation through inhibiting inflammation via activation of Nrf2. *EBioMedicine*. 2020;57:102832. doi:10.1016/j.ebiom.2020.102832
12. Xu W, Chao Y, Liang M, et al. CTRP13 mitigates abdominal aortic aneurysm formation via NAMPT1. *Mol Ther*. 2021;29:324–337. doi:10.1016/j.ymthe.2020.09.009
13. Buchmann GK, Schurmann C, Spaeth M, et al. The hydrogen-peroxide producing NADPH oxidase 4 does not limit neointima development after vascular injury in mice. *Redox Biol*. 2021;45:102050. doi:10.1016/j.redox.2021.102050
14. Peterss S, Mansour AM, Ross JA, et al. Changing pathology of the thoracic aorta from acute to chronic dissection: literature review and insights. *J Am Coll Cardiol*. 2016;68:1054–1065. doi:10.1016/j.jacc.2016.05.091
15. Wong KHF, Zucker BE, Wardle BG, et al. Systematic review and narrative synthesis of surveillance practices after endovascular intervention for lower limb peripheral arterial disease. *J Vasc Surg*. 2022;75:372–380 e315. doi:10.1016/j.jvs.2021.08.062
16. Narula N, Olin JW, Narula N. Pathologic disparities between peripheral artery disease and coronary artery disease. *Arterioscler Thromb Vasc Biol*. 2020;40:1982–1989. doi:10.1161/ATVBAHA.119.312864
17. Narula N, Dannenberg AJ, Olin JW, et al. Pathology of peripheral artery disease in patients with critical limb ischemia. *J Am Coll Cardiol*. 2018;72:2152–2163. doi:10.1016/j.jacc.2018.08.002
18. Matsuo Y, Takumi T, Mathew V, et al. Plaque characteristics and arterial remodeling in coronary and peripheral arterial systems. *Atherosclerosis*. 2012;223:365–371. doi:10.1016/j.atherosclerosis.2012.05.023
19. Dalager S, Falk E, Kristensen IB, Paaske WP. Plaque in superficial femoral arteries indicates generalized atherosclerosis and vulnerability to coronary death: an autopsy study. *J Vasc Surg*. 2008;47:296–302. doi:10.1016/j.jvs.2007.10.037
20. Ho CY, Shanahan CM. Medial arterial calcification: an overlooked player in peripheral arterial disease. *Arterioscler Thromb Vasc Biol*. 2016;36:1475–1482. doi:10.1161/ATVBAHA.116.306717
21. Patop IL, Wust S, Kadener S. Past, present, and future of circRNAs. *EMBO J*. 2019;38:e100836. doi:10.15252/embj.2018100836
22. Yu T, Wang Y, Fan Y, et al. CircRNAs in cancer metabolism: a review. *J Hematol Oncol*. 2019;12:90. doi:10.1186/s13045-019-0776-8
23. Huang A, Zheng H, Wu Z, et al. Circular RNA-protein interactions: functions, mechanisms, and identification. *Theranostics*. 2020;10:3503–3517. doi:10.7150/thno.42174
24. Gu Y, Ke G, Wang L, et al. Altered expression profile of circular RNAs in the serum of patients with diabetic retinopathy revealed by microarray. *Ophthalmic Res*. 2017;58:176–184. doi:10.1159/000479156
25. Zheng J, Li Z, Wang T, et al. Microarray expression profile of Circular RNAs in plasma from primary biliary cholangitis patients. *Cell Physiol Biochem*. 2017;44:1271–1281. doi:10.1159/000485487
26. Wu J, Li J, Liu H, et al. Circulating plasma circular RNAs as novel diagnostic biomarkers for congenital heart disease in children. *J Clin Lab Anal*. 2019;33:e22998. doi:10.1002/jcla.22998
27. Steinberg D. In celebration of the 100th anniversary of the lipid hypothesis of atherosclerosis. *J Lipid Res*. 2013;54:2946–2949. doi:10.1194/jlr.R043414
28. Zhang S, Li L, Chen W, et al. Natural products: the role and mechanism in low-density lipoprotein oxidation and atherosclerosis. *Phytother Res*. 2021;35:2945–2967. doi:10.1002/ptr.7002
29. Khatana C, Saini NK, Chakrabarti S, et al. Mechanistic insights into the oxidized low-density lipoprotein-induced atherosclerosis. *Oxid Med Cell Longev*. 2020;2020:5245308. doi:10.1155/2020/5245308
30. Sitia S, Tomasoni L, Atzeni F, et al. From endothelial dysfunction to atherosclerosis. *Autoimmun Rev*. 2010;9:830–834. doi:10.1016/j.autrev.2010.07.016
31. Gimbrone MA, Garcia-Cardena G. Endothelial cell dysfunction and the pathobiology of atherosclerosis. *Circ Res*. 2016;118:620–636. doi:10.1161/CIRCRESAHA.115.306301

32. Hansson GK, Robertson AK, Soderberg-Naucler C. Inflammation and atherosclerosis. *Annu Rev Pathol*. 2006;1:297–329. doi:10.1146/annurev.pathol.1.110304.100100
33. Garcia C, Blesso CN. Antioxidant properties of anthocyanins and their mechanism of action in atherosclerosis. *Free Radic Biol Med*. 2021;172:152–166. doi:10.1016/j.freeradbiomed.2021.05.040
34. Forstermann U, Xia N, Li H. Roles of vascular oxidative stress and nitric oxide in the pathogenesis of atherosclerosis. *Circ Res*. 2017;120:713–735. doi:10.1161/CIRCRESAHA.116.309326
35. Li B, Xia Y, Hu B. Infection and atherosclerosis: TLR-dependent pathways. *Cell Mol Life Sci*. 2020;77:2751–2769. doi:10.1007/s00018-020-03453-7
36. Souilhol C, Serbanovic-Canic J, Fragiadaki M, et al. Endothelial responses to shear stress in atherosclerosis: a novel role for developmental genes. *Nat Rev Cardiol*. 2020;17:52–63. doi:10.1038/s41569-019-0239-5
37. Peiffer V, Sherwin SJ, Weinberg PD. Does low and oscillatory wall shear stress correlate spatially with early atherosclerosis? A systematic review. *Cardiovasc Res*. 2013;99:242–250. doi:10.1093/cvr/cvt044
38. Lei M, Zheng G, Ning Q, et al. Translation and functional roles of circular RNAs in human cancer. *Mol Cancer*. 2020;19:30. doi:10.1186/s12943-020-1135-7
39. Zhang X, Wang P, Yuan K, et al. Hsa_circ_0024093 accelerates VSMC proliferation via miR-4677-3p/miR-889-3p/USP9X/YAP1 axis in in vitro model of lower extremity ASO. *Mol Ther Nucleic Acids*. 2021;26:511–522. doi:10.1016/j.omtn.2021.07.026
40. Zhou WY, Cai ZR, Liu J, et al. Circular RNA: metabolism, functions and interactions with proteins. *Mol Cancer*. 2020;19:172. doi:10.1186/s12943-020-01286-3
41. Qadir J, Li F, Yang BB. Circular RNAs modulate Hippo-YAP signaling: functional mechanisms in cancer. *Theranostics*. 2022;12:4269–4287. doi:10.7150/thno.71708
42. Zhang MW, Zhu ZH, Xia ZK, et al. Comprehensive circRNA-microRNA-mRNA network analysis revealed the novel regulatory mechanism of Trichosporon asahii infection. *Mil Med Res*. 2021;8:19. doi:10.1186/s40779-021-00311-w
43. Li S, Teng S, Xu J, et al. Microarray is an efficient tool for circRNA profiling. *Brief Bioinform*. 2019;20:1420–1433. doi:10.1093/bib/bby006
44. Xu X, Zhang J, Tian Y, et al. CircRNA inhibits DNA damage repair by interacting with host gene. *Mol Cancer*. 2020;19:128. doi:10.1186/s12943-020-01246-x